Isolated Three-phase AC to DC converter with Matrix Converter Applying Wide Output Voltage Operation

Jun-ichi Itoh
Dept. of Electrical, Electronics, and Information Engineering
Nagaoka University of Technology
Nagaoka, Japan
itoh@vos.nagaokaut.ac.jp

Satoshi Nakamura
Dept. of Electrical, Electronics, and Information Engineering
Nagaoka University of Technology
Nagaoka, Japan
s_nakamura@stn.nagaokaut.ac.jp

Shunsuke Takuma
Dept. of Electrical, Electronics, and Information Engineering
Nagaoka University of Technology
Nagaoka, Japan
takuma_s@stn.nagaokaut.ac.jp

Hiroki Watanabe
Dept. of Electrical, Electronics, and Information Engineering
Nagaoka University of Technology
Nagaoka, Japan
hwatanabe@vos.nagaokaut.ac.jp

***Abstract*— This paper proposes an expanded method of the output voltage control region of an isolated AC-DC converter utilizing multi-current mode operation for rapid battery charger applications. The rapid battery chargers require wide DC voltage regulation depending on the battery condition. On the other hand, the AC-DC converter which is composed by a dual active bridge matrix converter has the limitation of the output DC voltage range due to the current mode such as the continuous current mode (CCM) and discontinuous current mode (DCM). In this paper, the relationship between the output power and the output DC voltage at each current mode is clarified by the equations. In addition, the expansion of the output DC voltage region is achieved by changing current mode condition. Finally, the experimental results demonstrates the validity of the proposed method. As a result, both CCM and DCM operation are evaluated when the boost ratio is changed from 0.7 to 1.2. In addition, the sinusoidal input current waveform was obtained by the proposed control.**

Keywords— three phase AC-DC converter, Matrix converter, rapid battery charger

I. INTRODUCTION

Recently, the electric vehicles (EV) and the plug-in hybrid vehicles (PHV) may become a trend of automotive technologies for environmental problem solution, and the rapid battery chargers are the key component to enhance the convenience for users. The rapid battery chargers have the following requirement, e.g., high conversion efficiency, galvanic isolation, miniaturization. In particular, the reduction of the weight and the size is important for easy installation and dissemination. Typically, the rapid battery charger consists of the three-phase PWM converter and the bidirectional isolated DC-DC converter such as the Dual Active Bridge (DAB) converter, and it has good performance for the PFC capability with low harmonic distortion [1]-[4]. However, the DC-link capacitor between the PWM rectifier and the inverter has a short life-time because an electrolytic capacitor is usually selected for DC-link capacitor. In addition, the initial charging circuit hinders miniaturization. On the other hand, the bidirectional AC-DC converter which has matrix converter and the medium-frequency transformer has been studied [5]-[11]. These circuit directly convert the three-phase AC to medium-frequency single-phase AC without the PWM converter and the Voltage Source Inverter (VSI). Therefore, a number of conversions is reduced to improve the conversion efficiency. In particular, it has advantage for the size reduction because a large inductor such as the grid-tied inductor and DC-link capacitor does not necessary.

Some control method for the matrix converter integrated with the isolated AC-DC converter has been proposed [5]-[11]. In Ref. [5], the optimal switching pattern has been proposed to achieve the minimum current ripple on the DC side. However, the input current still distorts by the incomplete cancelation of the current ripple. In addition, the input current ripple increases compared with the conventional control scheme. In Ref. [6], the control method using DCM is mentioned. The advantage of this method is that the control algorism is easy owing to the simplification of the duty calculation by DCM. On the other hand, the output voltage control is necessary in order to regulate the battery voltage, and the voltage feedback control is implemented to the typical DAB converter in this system. Likewise, the isolated AC-DC converter with the matrix converter also requires the output voltage control for the battery voltage management. However, the output voltage region depends the power transferable , and the power transferable area depends CCM and DCM associated with the buck-boost inductance value at the each step-up ratio. Therefore, most of the conventional methods are applied to only the buck mode.

In this paper, the expansion method of the output voltage regulation range for the isolated AC-DC converter with the matrix converter is proposed. The originality of this paper is that the clarification of the output voltage range using the relationship between the output power and the output DC voltage at CCM or DCM current mode. In particular, the control method combined with CCM and DCM is introduced in order to expand the output voltage range. Finally, In the experimental result, the rated operation (1 p.u. = 6 kW) is demonstrated that the input current THD was less than 5% at the boost ratio from 0.7 to 1.2. The wide output voltage control

is possible by changing the current mode according to the boost ratio and output power.

II. Circuit Configration And Control Method

Figure 1 shows the circuit configuration of the bidirectional isolated AC-DC converter. This circuit is based on the three-phase to single-phase matrix converter and the DAB converter, and the matrix converter is installed on the primary side instead of the H-bridge inverter. The matrix converter directly converts the grid frequency to medium-frequency AC in order to minimize the transformer. In this circuit, a large inductor such as the grid-tied inductor and the DC output inductor does not necessary. Therefore, it is possible to reduce the system volume in comparison with typical circuit using BTB configuration.

Figure 2 shows the fundamental voltage vector diagram and the current vector I_{in}^*. In the matrix converter, in order to output the input current command in a sinusoidal shape, space vector modulation (SVM) is used so that the average output current in each switching cycle is constant. V_1 is the maximum phase voltage, and V_2 is the intermediate phase voltage of the line voltage. In addition, I_1 and I_2 are two vectors close to the current command vector and have a cycle of six times the grid voltage. Outputting the input current command I_{in}*, the input current is controlled by outputting I_1 and I_2 during V_1 and V_2 vector output. In order to obtain the medium-frequency voltage, V_1 and V_2 are output in the first half of the cycle, and then the inverse vectors V_4 and V_5 are output in the second half of the cycle.

However, In the bidirectional isolated AC-DC converter with matrix converter, the leakage inductance of the transformer smoothes the current. As a result, the inductance value is very small that a large ripple current occurs within the switching cycle. This problem increases the distortion of the input current and output current. Therefore, this converter is necessary to eliminate the ripple current. Figure 3 shows a medium-frequency current waveform with the current ripple cancellation method [7]. The ripple cancelation method is achieved by the selection of suitable output vector which is employed by the conventional SVM. The amplitude of the current vector during the power transmission period is made equal to the medium-frequency current command value I_{ave}^* by changing the output order of the negative voltage vector. As a result, the ripple current is equivalently neglected in the switching cycle, therefore the distortion of the input current and the output current without ripple can be achieved. The operation modes are separated into two modes such as buck mode and boost mode depending on the grid voltages and DC voltage. In addition, the output vector is selected with the consideration of the minimization of the reactive current. The sign function is defined as

$$sign(x)=\begin{cases}1 & x>NV_{dc}\\ -1 & x<NV_{dc}\end{cases} \qquad x=\frac{v_1I_1+v_2I_2}{I_1+I_2} \qquad \text{.....(1).}$$

The average current I_{ave} during point A to B is defined as the equivalent transformer current reference I_{ave}^* in the powering mode. Each duty of I_1 and I_2 expressed as

$$D_1=\frac{I_1}{I_{ave}^*}-sign(x)D_z \qquad \text{.....(2),}$$

$$D_2=\frac{I_2}{I_{ave}^*} \qquad \text{.....(3),}$$

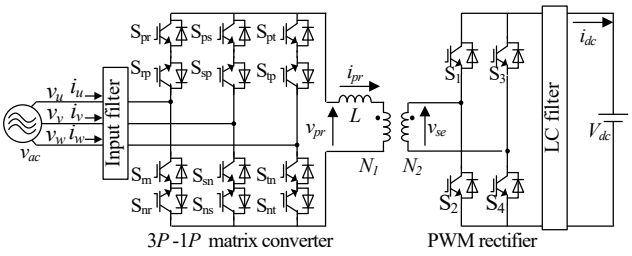

Fig. 1. Bidirectional isolated AC-DC converter with matrix converter.

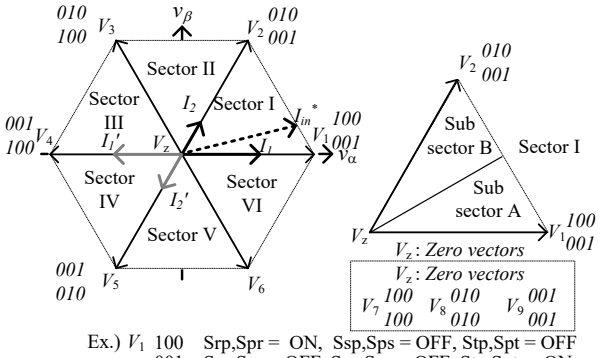

(a) Space vector modulation

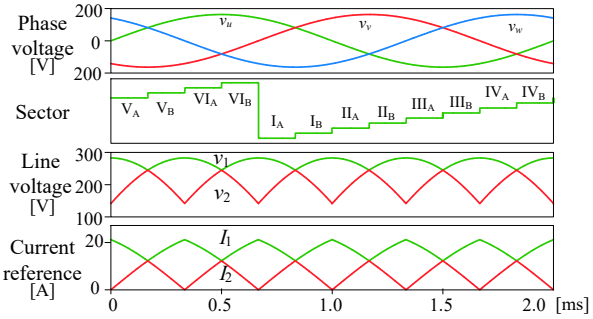

(b) Relationship between grid voltage and current reference

Fig. 2. Fundamental space vector diagram.

where D_z is the compensation duty for D_1. The current during D_z is a reactive or active current in the buck or boost mode. Therefore, to compensate for the effect of the current in D_z, an addition or subtraction from D_1 is required and is expressed as

$$2\frac{(v_1+NV_{dc})}{L}T(D_\alpha-\frac{1}{2}D_z(1+sign(x))) +\frac{(v_1-NV_{dc})}{L}TD_1+\frac{(v_2-NV_{dc})}{L}TD_2=2I_{ave}^* \qquad \text{..... (4)}$$

where L is the leakage inductance referred to the primary side of the transformer, V_{dc} is the DC voltage. In the equation (3), D_a is expressed as

$$D_\alpha=\frac{2I_{ave}^*\frac{L}{T}-(v_1-NV_{dc})D_1-(v_2-NV_{dc})D_2}{2(v_1+NV_{dc})} -\frac{1}{2}D_z(1+sign(x)) \qquad \text{(5).}$$

D_z is decided to equalize the amount of the change during T_1 to T_2 respectively.

$$D_z = sign(x)\frac{(v_1 - NV_{dc})I_1 + (v_2 - NV_{dc})I_2}{2NV_{dc}I_{ave}^*} \quad \text{... (6)}$$

Substring (6) into (1), D_1 is expressed by

$$D_1 = \left\{\frac{I_1}{I_{ave}^*}\frac{(V_2 - V_{out})D_2}{V_1 + V_{out}}\right\}\frac{(V_1 + V_{out})}{2V_{out}} \quad \text{..... (7)}$$

Finally, the zero current period D_0 is defined by

$$D_0 = 1 - (2D_\alpha + D_1 + D_2 + D_z) \quad \text{..... (8)}$$

The equivalent transformer current reference I_{ave}^* is restricted by the switching frequency, the leakage inductance L, the grid voltage, and the DC voltage. The equivalent transformer current reference is expressed as

$$I_{ave}^* = \frac{1}{2}\left\{(1 - D_0)\frac{v_1 + NV_{dc}}{2}\frac{T}{L} - \sqrt{K_1 - K_2}\right\}. \quad (9)$$

$$\because \left(\frac{v_1 + NV_{dc}}{2}\frac{T}{L}\right)$$

$$K_2 = \frac{v_1 + NV_{dc}}{2}\frac{I_1(v_1 + NV_{dc}) + I_2(v_2 + NV_{dc})}{NV_{dc}}\frac{T}{L}$$

The current references for CCM and DCM are same at the boundary condition. The output power at the boundary condition is expressed as

$$P_{b\_buck} = \frac{V_{out}}{2\sqrt{6}V_{ac}}\left(\frac{3}{2}V_{ac}^2 - V_{out}^2\right)\frac{T}{L} \quad \text{..... (10)},$$

$$P_{b\_boost} = \frac{\pi v_{ac}}{2\sqrt{2}NV_{dc}}\frac{N^2V_{dc}^2 - 2v_{ac}^2}{\omega L} \quad \text{..... (11)}$$

where V_{ac} is the RMS value of the grid voltage. The equations (10) and (11) express the boundary condition without CCM during 0 to 30 degree completely. Solving (9), the maximum output power *Pout* is expressed as

$$P = \frac{\pi\sqrt{6}}{8}\frac{v_{ac}NV_{dc}}{\omega L} \quad \text{..... (12)}$$

Changing (12), the leakage inductance is calculated by using (13).

$$L \le \frac{\pi\sqrt{6}}{16}\frac{v_{ac}NV_{dc}}{\omega P} \quad \text{..... (13)}$$

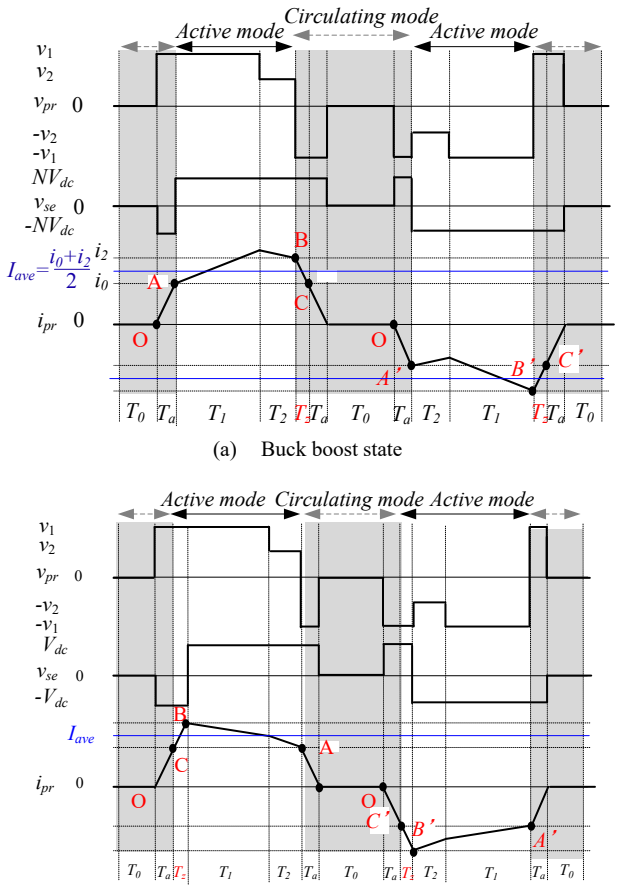

Fig. 3. Ripple cancellation method in order to simplify the duty calculation and minimize the reactive power.

Figure 4 shows the relationship between the output power and the ratio of the input and output voltage. CCM and DCM are used to realize the boost and buck operation. According to (12), the output power is restricted by the switching frequency, the leakage inductance, the grid voltage, the DC voltage, and the turn ratio. The DAB converter for the DC-DC conversion has the similar limitation by the same circuit parameter. The medium-frequency current has zero current period in DCM when the DC voltage is significantly larger or lower than the grid voltage at a light load.

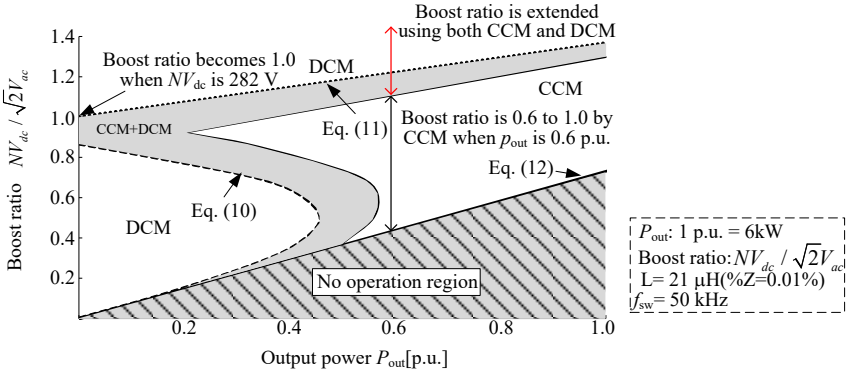

Fig. 4. Relationship between output power and boost ratio. The operation mode and current mode are changed by the grid voltage, DC voltage and transition power. Each line means the boundary condition to operate the proposed converter at CCM and DCM.

III. Commutation Error Compensation Method On Ripple Cancellation Method

A. *Voltage error caused due to 4-step voltage commutation*

The matrix converters need switching that prevents short circuits in the power supply and does not open the load with inductive loads. As a method of commutating, while satisfying this condition, there is a voltage commutation method that commutates depending on the magnitude of the voltage and a current commutation method that requires the direction of the load current. However, the load current has a medium-frequency, the current commutation method requires a highly accurate current sensor, which increases the cost. Therefore, in this study, we apply a 4-step voltage commutation that does not require a current sensor.

Figure 5 shows the model of voltage commutation using a bidirectional switch and the switching sequence. When the current direction is positive ($i_{load} > 0$) and commutation is made from the power supply v_a to v_b, consider the case where S_{1a} and S_{1b} are ON and S_{2a} and S_{2b} are OFF under the conditions of $v_a > v_b$. At this time, the switching sequence is executed in the order of S_{2a}:ON, S_{1a}:OFF, S_{2b}:ON, S_{1b}:OFF. At this time, commutation from v_a to v_b occurs when S1a in the second step is turned off. That is, the output voltage is delayed from the ideal timing by the dead time Td. Similarly, when commutating from the power supply v_a to v_b under the condition of $v_a < v_b$, the commutation from v_a to v_b occurs in the third step, so the actual output voltage is delayed by 2 Td. Therefore, the delay of the output voltage due to commutation is not always constant and is determined by the voltage condition and the current direction, so it is necessary to compensate for the duty considering the delay.

B. *Voltage commutation compensation during DCM operation under boost condition*

Figure 6 shows the operation waveforms of ideal commutation and voltage commutation in DCM. the voltage magnitude relationship is $v_u > v_v > v_w$. In the ripple cancel method, the drive mode as DCM in the light load region and CCM in the heavy load region. During the power transmission period, duty is generated so that the amplitude of the current vector becomes equal to the medium-frequency current command value i_{ave}^* in each cycle. However, voltage commutation causes a delay in the output voltage due to commutation. Fig. 6(b) shows the outline of operation considering the delay of the output voltage due to commutation. For example, when commutating from T_0 (V_9) to T_b (V_4), the voltage is commutated from the w phase to the u phase, which is the commutation from the minimum voltage phase to the maximum phase. Since the current direction is positive, the commutation delay is $2T_d$. Then, when commutating from T_b (V_4) to T_2 (V_5), it is commutation of the voltage from u phase to v phase, and it is commutation from the maximum voltage phase to the intermediate phase. Since the current direction is positive, the delay due to the commutation of the voltage is T_d. In other words, the output voltage period of T_b(V_4) is shortened by T_d due to commutation. As a result, the current average value i_{ave} does not match the command value. In particular, since the inductor voltage during the T_b period is higher than in other periods, the error due to the dead time greatly affects the error between the transmitted power and the command. Moreover, since the voltage during the ideal period is not output, the medium-frequency initial current is not held at zero. This causes distortion in the input current because it does not meet

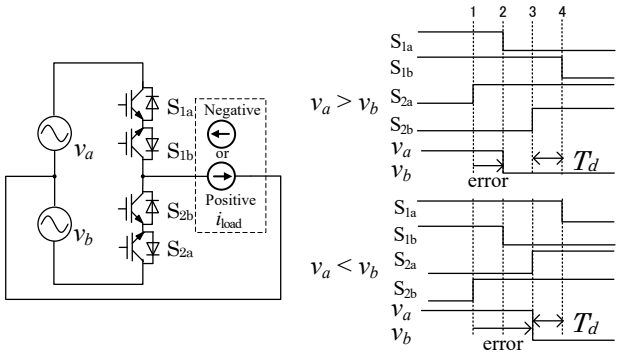

Fig. 5. Commutation model and voltage error.

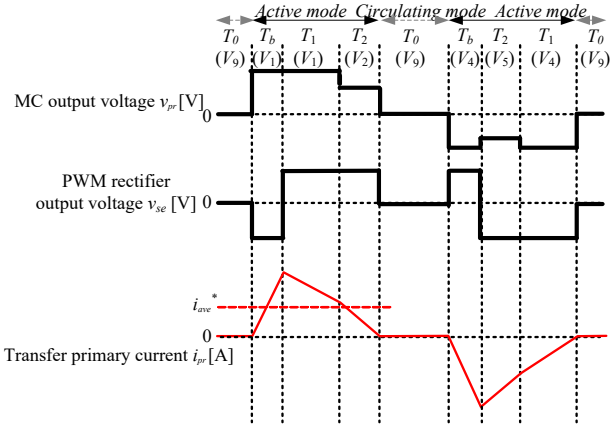

(a) Ideal commutation

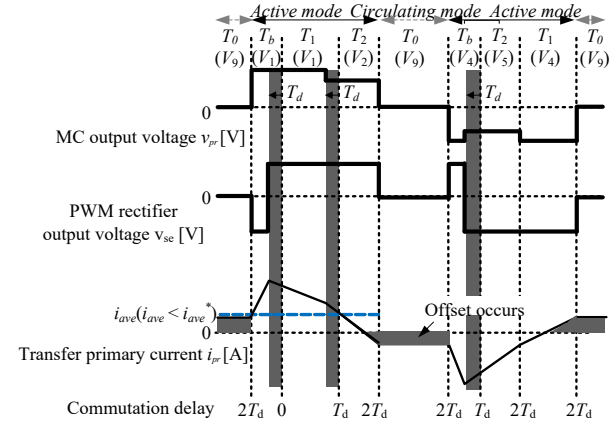

(b) Voltage commutation

Fig. 6. Comparing the operation mode around the DCM operation.

the DCM duty calculation assumptions. Therefore, we consider a method of compensating for voltage errors due to commutation.

Regarding the voltage error compensation amount during DCM operation, the error in the output voltage due to commutation is shortened by T_d during the period of T_b and extended by T_d during the period of T_2as shown in Fig. 7(b). When expressed by, it becomes equation (14).

$$\begin{cases} T_b^{'} = T_b + T_d \\ T_2^{'} = T_2 - T_d \end{cases} \quad \text{.....(14)}$$

C. *Voltage commutation compensation during CCM operation under boost condition*

In the ripple cancellation method, the drive mode as DCM in the light load region and CCM in the heavy load region. However, the system changes at 300 Hz, so the duty also changes at 300 Hz cycles. Depending on the operating conditions, a period in which DCM and CCM coexist at a 300 Hz cycle occurs.

Figure 7 shows the CCM operation waveforms in the region close to DCM and the heavy load region. In Fig. 7(a), the output period of Ta is shorter than the dead time, and the problem occurs that the medium-frequency current direction reverses before the voltage vector switches. When the dead time error compensation is applied, the current direction in which the voltage vector switches before and after compensation is different, and the voltage error due to commutation changes the compensation amount before and after compensation. Further, when the inductor current becomes zero during the commutation period, a voltage polarity reversal phenomenon occurs in which the polarity of the transformer voltage is reversed. From the above, it is not possible to compensate for the output voltage error due to the region in which the current direction is reversed [12].

Therefore, the proposed method of compensating for the nonlinear power error due to the voltage polarity reversal phenomenon by using the voltage waveform including the zero voltage period. The current direction reversal phenomenon is suppressed by providing a zero current period in the inductor current and controlling the zero current periods beyond the dead time. The current command i_{ave}^* is expressed by equation (15).

$$I_{ave}^* = \frac{1}{2}\left\{K_{cof1} - \sqrt{(K_{cof1}^2 - K_{cof2})}\right\} \quad \text{.....(15)}$$

$$\because \quad \frac{v_1 + NV_{dc}}{2}\frac{T}{L}$$

$$K_{cof2} = \frac{v_1 + NV_{dc}}{2}\frac{\{I_1(3NV_{dc} - v_1) + I_2(3NV_{dc} - v_2)\}T}{NV_{dc}L}$$

Further, the calculation formula of each duty is expressed by the formulas (16) to (21) using the current command i_{ave}^* of the formula (15).

$$T_1 = \left\{\frac{I_1}{I_{ave}^*} + \frac{(V_2 - V_{out})D_2}{V_1 + V_{out}}\right\}\frac{(V_1 + V_{out})}{2V_{out}} \quad \text{.....(16)}$$

$$T_2 = \frac{I_2}{I_{ave}^*} \quad \text{.....(17)}$$

$$T_z = \left(\frac{(NV_{dc} - v_1)I_1}{I_{ave}^*} + T_2(NV_{dc} - v_2)\right)\frac{1}{2NV_{dc}} \quad \text{.....(18)}$$

$$T_\alpha = \frac{2I_{ave}^* Lf_{sw} - (v_1 - NV_{dc})T_1 - (v_2 - NV_{dc})T_2}{2(v_1 + NV_{dc})} - T_z \quad \text{.....(19)}$$

$$T_b = T_a + T_z \quad \text{.....(20)}$$

$$T_0 = 1 - (T_1 + T_2 + T_a + T_b) \quad \text{.....(21)}$$

By driving with DCM, the current direction when switching each voltage vector does not change from that of DCM used with a light load. Therefore, the voltage error due to commutation is constant in the switching cycle, and power error compensation is possible. However, there is a drawback that the number of times of switching increases because the number of times of switching the voltage vector increases. The voltage error compensation amount is given by equation (22) and (23). Expression (23) is the compensation amount when the direction of the medium-frequency current i_{pr} is negative.

$$\begin{cases} T_b' = T_b + T_d \\ T_0' = T_0 - T_d \end{cases} \quad \text{.....(22)}$$

$$\begin{cases} T_1' = T_1 + T_d \\ T_2' = T_2 - T_d \end{cases} (i_{pr} < 0) \quad \text{.....(23)}$$

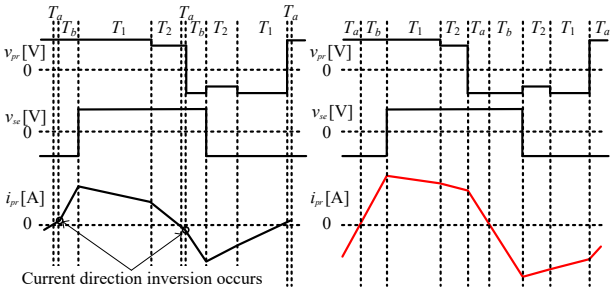

(a) Around the DCM (b) Heavy load area

Fig. 7. Outline of the CCM operation.

Table 1. Experimental parameters.

Quantity	Symbol	Value
Rated power	P	6.0 kW
Three-phase AC voltage	v_{ac}	200 V
DC voltage	V_{dc}	Max 100 V
Input frequency	f	50 Hz
Carrier frequency	f_{sw}	50 kHz
Leakage inductance	L	21 μH
Turn ratio of transformer	N_1:N_2	3.3:1
Input filter	L_f	0.19 mH
	C_f	10 μF
Dead-time	T_d	250 ns

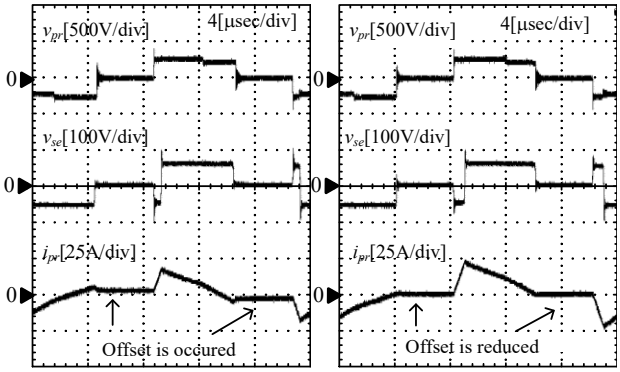

(a) Without compensation (b) With compensation

Fig. 8. Waveforms of matrix converter and rectifier.

IV. Experimental Verification

Fig. 8(a) shows the primary side voltage, current, and secondary side voltage in the conventional DCM region, and Fig. 8(b) shows the primary side voltage, current, and secondary side voltage with power error compensation. The transmission power command at this time is 2000 W. From Fig. 8(a), in the conventional method, an error occurs in the output voltage due to the commutation operation of the

matrix converter, and an offset occurs in the medium-frequency current during the period when the current is essentially zero. On the other hand, as shown in Fig. 8(b), the medium-frequency current also converges to zero in synchronization with the zero voltage period by suppressing the output voltage error by error compensation.

Figure 9 shows the input/output characteristics in the DCM region before and after voltage error compensation. In Fig. 9(a), it was seen that the initial current, which is the premise of the duty calculation in the DCM, which does not satisfy the condition of zero, and that the input current is greatly distorted. In Fig. 9(b), it was confirmed that by suppressing the offset that was superimposed on the medium-frequency current, the assumption of the ripple cancellation method that the initial current was zero was satisfied, and the input current distortion could be reduced.

Figure 10 shows a comparison diagram of the proposed DCM operation and the CCM operation waveform with the current direction reversed. In CCM operation, as shown in Fig. 7(a), the current direction is reversed before the voltage vector is switched, so the power compensation becomes non-linear and difficult to compensate. On the other hand, in the DCM operation proposed in <3.C>, the medium-frequency current converges to zero in the zero voltage period, so the current direction does not change when the voltage vector changes.

Figure 11,12 shows the input/output characteristics and waveforms of matrix converter and rectifier at the rated conditions under the boost ratio of 0.7, 0.866.1.0, and 1.2. It was confirmed that the system voltage and current are in phase and controlled at THD 5.0% or less under each boost condition while controlling at a power factor of 1. Also, it is clear that the theoretical medium-frequency voltage is generated and the slope of the current is controlled.

A ripple component of 300 Hz cycle generates on the output current near the zero current of each phase current. The duty of T_2 that outputs the intermediate phase always zero at the timing when the current of each phase becomes zero, and there is a range in which the pulse width is shorter than the dead time. As a result, a pulse drop is generated near the zero current of each phase, and as a result, the voltage vector that should be output is not output. This is because the duty of T_2 that outputs the intermediate phase is always zero at the timing when the current of each phase is zero, and there is a range in which the pulse width is shorter than the dead time. As a result, a pulse drop generates near the zero current of each phase, and the voltage vector to be output is not output.

Figure 13 shows the THD characteristics. The THD at the rated value is below 5% under any boost condition. However, the input current distortion still tends to be large at light loads. This is because the range of pulse deficiency in the period T2 during which the intermediate phase is output becomes wider at light load, and the effect of dead time becomes larger relative to the fundamental wave.

Figure 14 shows the efficiency characteristics. The maximum efficiency point reaches 96.7% at 1.5 kW output under the condition of step-up ratio 0.866. The efficiency tends to decrease after 3 kW under any boosting condition. This problem is solved by changing the maximum efficiency point by optimal design of the transformer and medium-frequency inductor.

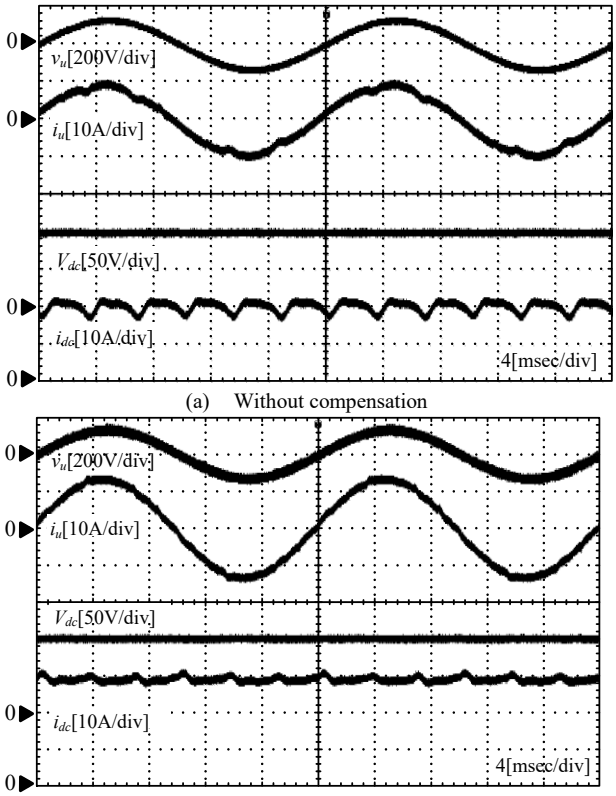

Fig. 9. Input and output waveforms on DCM.

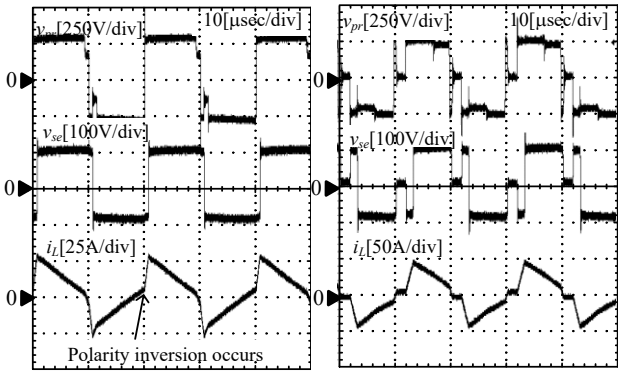

Fig. 10. Comparing the operation mode around the DCM operation.

V. CONCLUSIONS

In this paper, the output voltage region of the isolated AC-DC converter with the matrix converter is proposed using the mathematical equation. The proposed method shows to operate the power transmission with a wide output voltage range. The originality point of the paper is to clarify the operating output voltage range using the relationship between the output power and the output DC voltage at each current mode. As the result, it was mentioned that the output voltage region under CCM and DCM is difference. In addition, transmission power error compensation to improve input current distortion under boost conditions. By analyzing the voltage error caused by commutation, the average value of the medium-frequency current during the transmission power period is approximated to the ideal value, and the offset is reduced in the medium-frequency current during the zero voltage period. The experimental results, the current THD at rated power operates at less than 5% in both step-down and step-up conditions, and the maximum efficiency value is 96.7%.

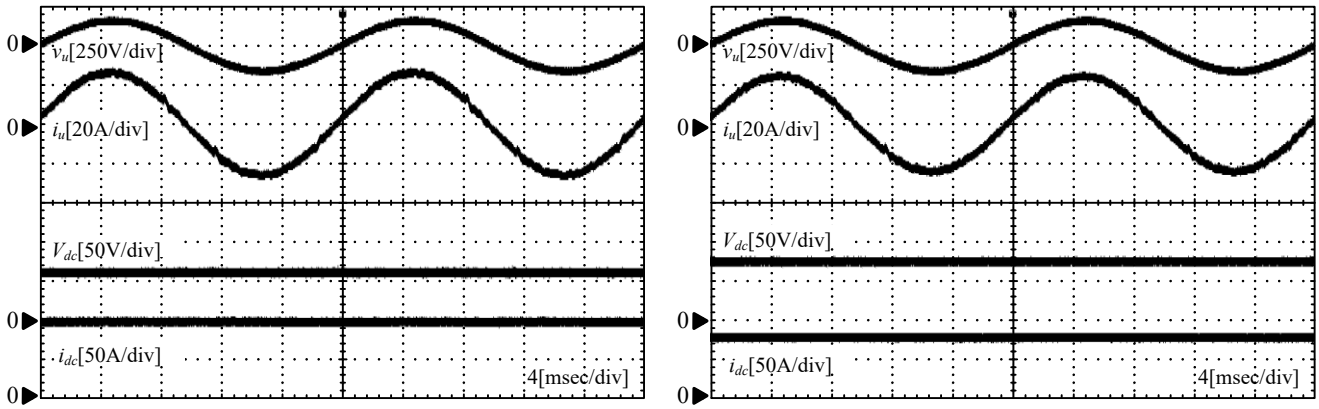

(a) Boost ratio 0.7. (b) Boost ratio 0.866

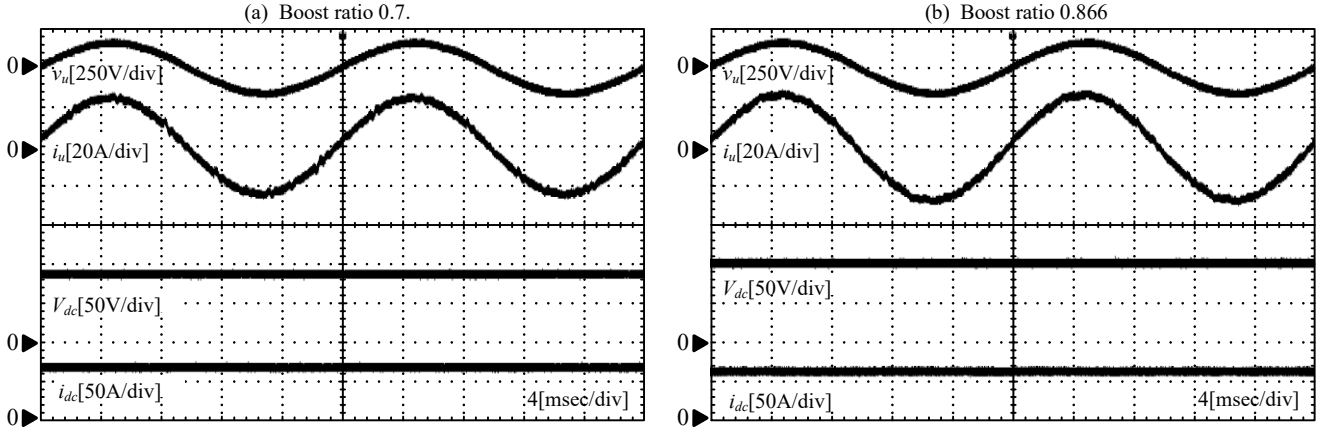

(c) Boost ratio 1.0. (d) Boost ratio 1.2.

Fig. 11. Input and output waveforms of matrix converter with rated operation

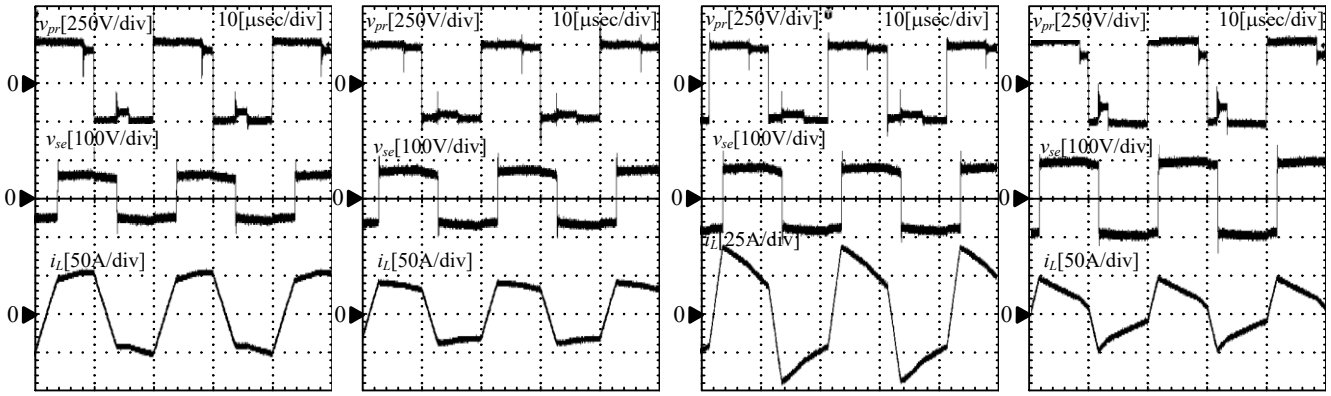

(a) Boost ratio 0.7. (b) Boost ratio 0.866 (c) Boost ratio 1.0. (d) Boost ratio 1.2.

(a) Fig. 12. Waveforms of matrix converter and rectifier with rated operation.

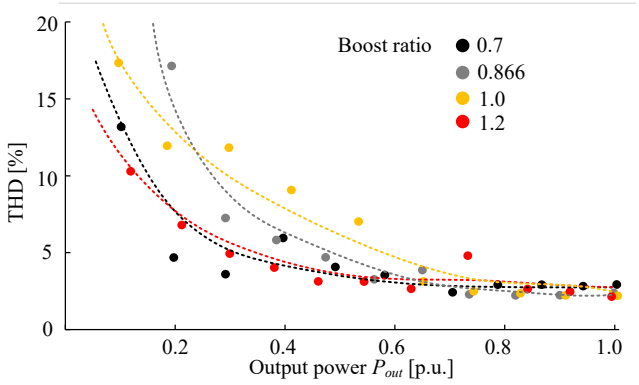

Fig. 13. THD characteristics.

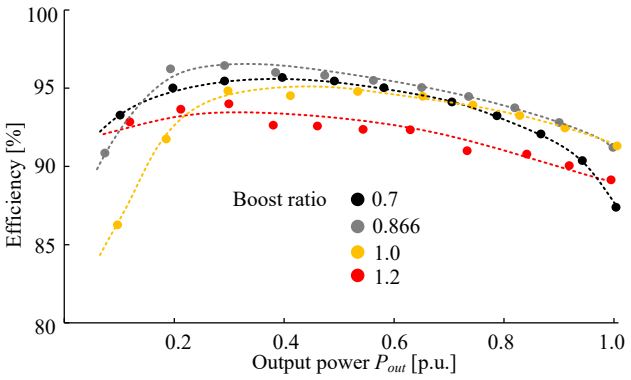

Fig. 14. Efficiency characteristics

REFERENCES

[1] Muhammad Hazarul Azmeer bin Ab Malek, Hiroaki Kakigano, and Kiyotsugu Takaba"Combined PulseWidth Modulation of Dual Active Bridge DC-DC Converter to Increase the Efficiency of Bidirectional PowerTransfer,"IEEJ Journal of Industry Applications, vol. 7, no. 2, pp. 166-174, (2018).

[2] Seiji Iyasu, Yuji Hayashi, Yuichi Handa, Kimikazu Nakamura, Keiji Wada, "A Bidirectional Current Sensor based on CT with Diode Rectifier and MOSFET for Bidirectional Current-fed DC-DC Converter" IEEJ Journal of Industry Applications, vol. 8, no. 3, pp. 437-443, (2019).

[3] Peiwen He, Alireza Khaligh "Comprehensive Analyses and Comparison of 1 kW Isolated DC–DC Converters for Bidirectional EV Charging Systems" IEEE Transactions on Transportation electrification, voL. 3, no. 1(2017)

[4] Seyed Amir Assadi, Hirokazu Matsumoto, Mazhar Moshirvaziri , Miad Nasr, Mohammad Shawkat Zaman, Olivier Trescases "Active Saturation Mitigation in High-Density Dual-Active-Bridge DC–DC Converter for On-Board EV Charger Applications" IEEE Transactions on Power Electronics vol. 35, no. 4, pp. 4376-4387, (2020).

[5] J. Afsharian, D. David Xu, B. Gong and Z. Yang, "Space vector demonstration and analysis of zero-voltage switching transitions in three-phase isolated PWM rectifier," 2015 IEEE Energy Conversion Congress and Exposition (ECCE), Montreal, , pp. 2477- 2484(2015)

[6] D. Das, N. Weise, K. Basu, R. Baranwal and N. Mohan, "A Bidirectional Soft-Switched DAB-Based Single-Stage Three-Phase AC–DC Converter for V2G Application," in IEEE Transactions on Transportation Electrification, vol. 5, no. 1, pp. 186-199, (2019).

[7] S. Takuma, K. Kusaka, J. Itoh, Y. Ohnuma, S. Miyawaki: "A Novel Current Ripple Cancellation PWM for Isolated Three-phase Matrix DAB AC-DC Matrix Converter", European Conference on Power Electronics and Applications (EPE) (2019)

[8] Lukas Schrittwieser, Michael Leibl, Johann W. Kolar, R. Baranwal and N. Mohan, "99% Efficient Isolated Three-Phase Matrix-Type DAB Buck-Boost PFC Rectifier" in IEEE Transactions on Power Electronics (2019).

[9] Mahmoud A. Sayed, Kazuma Suzuki, Takaharu Takeshita,"PWM Switching Technique for Three-Phase Bidirectional Grid-Tie DC–AC–AC Converter With High-frequency Isolation" IEEE Transactions on Power Electronics, voL: 33, Issue: 1, Jan. (2018)

[10] Keping You ; Dan Xiao ; Muhammed Fazlur Rahman ; M. Nasir Uddin "Applying Reduced General Direct Space Vector Modulation Approach of AC–AC Matrix Converter Theory to Achieve Direct Power Factor Controlled Three-Phase AC–DC Matrix Rectifier" IEEE Transactions on industry applications, voL. 50, no. 3(2014)

[11] Prathamesh Pravin Deshpande, Amit Kumar Singh, Hau Chong Aih, Sanjib Kumar Panda, "A Matrix-based Isolated Bidirectional AC-DC Converter with LCL type Input Filter for Energy Storage Applications" IEEJ Journal of Industry Applications, vol. 8, no.4, pp. 644-651, (2019)

[12] K. Takagi and H. Fujita, "Dynamic control and dead-time compensation method of an isolated dual-active-bridge DC-DC converter," 2015 17th European Conference on Power Electronics and Applications (EPE'15 ECCE-Europe), Geneva, 2015, pp. 1-10